

Discrete Fracture Network Generation for the Äspö TAS08 Tunnel using MoFrac

Junkin, W., Janeczek, D., Bastola, S., Wang, X., Cai, M. and Fava, L.

MIRARCO Mining Innovation, Sudbury, Ontario, Canada

Sykes, E.

Nuclear Waste Management Organization, Toronto, Ontario, Canada

Munier, R.

Swedish Nuclear Fuel and Waste Management Co., Stockholm, Sweden

Srivastava, R.M.

FSS Canada Consultants Inc., Toronto, Ontario, Canada

Copyright 2017 ARMA, American Rock Mechanics Association

This paper was prepared for presentation at the 51st US Rock Mechanics / Geomechanics Symposium held in San Francisco, California, USA, 25-28 June 2017. This paper was selected for presentation at the symposium by an ARMA Technical Program Committee based on a technical and critical review of the paper by a minimum of two technical reviewers. The material, as presented, does not necessarily reflect any position of ARMA, its officers, or members. Electronic reproduction, distribution, or storage of any part of this paper for commercial purposes without the written consent of ARMA is prohibited. Permission to reproduce in print is restricted to an abstract of not more than 200 words; illustrations may not be copied. The abstract must contain conspicuous acknowledgement of where and by whom the paper was presented.

ABSTRACT: This paper presents a validation study for a new software tool, MoFrac, which generates realistic discrete fracture network (DFN) models. MoFrac implements aspects of a unique geostatistical and rules-based methodology for DFN generation. Non-planar fractures are generated through a conditional simulation process that propagates deterministic fracture traces in three dimensions. Stochastic fractures are generated based on conditioning to statistics derived from field-mapped fracture traces and orientation parameters. Data mapped from the Äspö TAS08 tunnel close to Oskarshamn, Sweden were used for this validation study. The generated DFN model was analyzed for fracture orientation, size, intensity, and location. The modeling results demonstrate that MoFrac generates representative DFNs with a realistic appearance that conform to mapped fracture traces and statistics derived from the input data. MoFrac DFNs are suitable for integration into a variety of numerical models.

1. INTRODUCTION

The dynamics of a rock mass are related to the occurrence of natural discontinuities which occur on different scales, with variable intensities, shapes, and distributions through space (Lei *et al.*, 2017). Fracture truncation, branching, clustering and spacing, among other measurable attributes, define the geometry of a fracture network. Computational models that represent the geometry of fracture networks contribute to the understanding of the strength and deformation behavior of rock masses, rock fragmentation, slope stability, groundwater flow, and mass transport. A discrete fracture network (DFN) model represents the geometric arrangement and characteristics of fractures within a volume of rock.

Several means of fracture network generation are described in the literature. Placement methods are computationally efficient because fractures are modeled as simple planar shapes arranged within a domain (Long *et al.*, 1985), but the realism and accuracy of resulting DFN models are often limited. Mechanical propagation methods can produce realistic DFNs by simulating the creation of fractures driven by complex geomechanical conditions. These models are generally limited to fracture

propagation in two dimensions and are computationally intensive (Lei *et al.*, 2014). Geometrical propagation methods (Srivastava, 2002) are employed by MoFrac and provide much of the realism of mechanical propagation methods, while remaining computationally efficient.

MoFrac DFN models are composed of both stochastic and deterministic fractures. Attributes that reflect properties of fracture groups are used to generate stochastic fractures at locations within a rock volume where no fracture data have been recorded. These statistical fracture group attributes are derived from available data such as orientation, size, and geological hierarchy, all of which are generally interpreted from mapped field data. Deterministic fractures are propagated from mapped fracture traces on ground surface or tunnel walls, guided by the actual trace and the applicable fracture group attributes, such as orientation and shape. This methodology, combining both types of fractures, supports DFN modeling of a rock mass with varying degrees of available data regarding the volume of interest. The accuracy, certainty, and realism of a DFN will be proportional to the quality and totality of the input data.

The MoFrac DFN software is developed by MIRARCO, based on the methodologies first implemented in FXSIM3D (Srivastava, 2002) for the generation of three-dimensional DFN models conditioned to the statistical attributes of any available mapped fracture data (Srivastava *et al.* 2004). MoFrac generates realistic fracture networks consisting of non-planar, undulated stochastic and deterministic fractures conditioned to both individual and group attributes. Successful DFN modeling has been accomplished using pre-beta versions of MoFrac (Vazaios *et al.*, 2014, 2015; Farahmand *et al.*, 2015; Macciotta & Martin, 2015).

This validation study assesses the capability of MoFrac to generate DFN models that honor mapped fracture data and fracture group attributes in underground excavations. Specifically, fracture orientation, intensity, size, and spatial location are quantitatively assessed.

2. DFN GENERATION METHODOLOGY IN MOFRAC

A fracture surface generated by MoFrac is represented as a mesh of approximately equilateral triangles. A fracture propagates from a mapped trace through tessellation of this mesh, guided by an orientation plane that is probabilistically derived and constrained by known data. During this process the fracture surface is undulated, controlled by input parameters. Deterministic fractures propagate from known fracture traces, whereas stochastic fractures propagate from probabilistically generated traces that conform to the statistical distribution and characteristics of the anticipated DFN.

Fractures are generated sequentially, from largest to smallest. Regions can be defined and deterministic fractures are modeled before stochastic fractures in each discrete region. This approach allows for stochastic infilling, when needed, in order to achieve a desired fracture intensity. Stochastic fractures can be prevented from intersecting defined surfaces or volumes, and can be prevented from crossing regional boundaries. Fracture groups are assigned truncation probabilities, geometric and spatial properties, and are sequenced based on user-defined rules. Scaling can be used to adjust the triangle size of a surface mesh according to fracture size. Alternatively, all fractures can be generated with the same resolution.

3. DFN PARAMETERS IN MOFRAC

MoFrac has a number of required parameters, such as fracture orientation, intensity, size, and undulation for DFN modeling. Input datasets may include fracture traces, lineaments, and surface meshes.

3.1. Fracture intensity and size distributions

Cumulative length distributions (CLD) and cumulative area distributions (CAD) can be used by MoFrac to characterize the number and size of fractures in defined fracture groups.

Fracture intensity attribute values can be two-dimensional (P_{21} , CLD) or three dimensional (P_{32} , CAD). These values are scale independent; however, P_{21} values are dependent on the orientation of fractures relative to the observation plane (Dershowitz & Herda, 1992). A cumulative length or area distribution can be interpreted on a log-log plot showing the number of fractures greater than a size threshold per domain (area or volume).

The number of stochastically generated fractures for a group in a defined region (N_s) is determined using the slope of the distribution on a log-log plot that shows the change in fracture intensity as a function of size, along with limiting minimum and maximum values. MoFrac generates fractures uniformly across a defined distribution, representing fracture size and intensity. The total number of stochastic fractures generated is the difference between the minimum and maximum size thresholds.

3.2. Fracture orientation

Fracture orientation is the attribute commonly used to define fracture groups. By viewing fracture orientation data on a stereonet, fracture groups can be identified. Orientations can be expressed using common nomenclature, (dip, dip direction, k), (strike, dip), or (trend, plunge), where k is Fisher's dispersion factor. Where a dispersion factor is not used, a standard deviation is assigned to each input fracture orientation individually.

3.3. Fracture undulation

Fractures are non-planar in situ. MoFrac provides an undulation feature intended to mimic the geometry of natural fracture surfaces. An undulated surface is created by assigning height values from a mean orientation plane, across the fracture surface. Deterministic fractures are forced to honor their natural undulation as sampled at the location of the trace. Stochastic fractures are seeded from an initial trace, randomly located, that has shape assigned through two parameters: fractal dimension, and the number of iterations.

The process of generating an undulating trace begins with a line segment which is fractalized using a technique derived from the h-L method (Li & Huang, 2015). Let D be the fractal dimension of the line and for every iteration of the fractalization, the length of the line increases to:

$$L' = L \cdot \left(\frac{2^D}{2}\right) \quad (1)$$

A line is inflected as many times as required to achieve the sinuosity satisfying the fractal dimension assigned. This creates a randomized wiggly line that can be

generated based on characteristics of mapped fracture traces.

The number of iterations is the second input parameter to create a stochastic trace. Every iteration uses line segments one half the length of the previous iteration. These simulated fracture traces are generated at randomized locations in the defined region, and then are propagated to form fracture surfaces using the same processes as deterministic fracture propagation.

The surface of the fracture is also undulated using the same process with a second fractal dimension input. This undulation occurs perpendicular to the trace and the number of iterations is determined by the fracture's dip length.

3.4. Additional DFN parameters

The actual shape and size of fractures in situ are unknown in three dimensional space (Jing & Stephansson, 2007). These attributes are characterized through three parameters: strike to dip ratio, shape, and a terminal area constraint (TAC) factor. The TAC factor specifies a range across the fracture surface where the associated trace could be situated. This process uses the ratio of fracture surface area on either side of a trace. A TAC factor of 1 means that traces always bisect the fracture shape. When a TAC factor greater than 1 is applied, a randomized value between 1 and the TAC factor is used, on a fracture-by-fracture basis. The strike to dip ratio and the TAC factor determine the size of a fracture based on the trace, and contribute to the resulting shape. The basic shape of a modeled fracture is elliptical or rectangular, as specified for the fracture group. Both shapes were considered for validation and the final DFN model presented is a randomized mix between the two fracture shapes.

Deterministic fractures have both individual and group orientations; in case these orientations conflict, the orientation honored is specified by an input parameter.

4. ÄSPÖ CASE STUDY

This case study was undertaken as a validation of the capability of MoFrac to generate realistic and geologically plausible DFN models. Modeling was completed using MoFrac Beta, build number 4570. Äspö Tunnel TAS08 is part of the SKB's HRL located 400 m below surface, oriented Northwest, with an approximate azimuth of 322°. The tunnel is about 7 m in height and is shown in plan view in Figure 1. The data for this modeling were collected by the Swedish Nuclear Fuel and Waste Management Company (SKB) at the Äspö Hard Rock Laboratory (HRL) near Oskarshamn, Sweden (SKB, 2016). Fracture traces were mapped on the Äspö TAS08 tunnel walls and are shown in Figure 2. A second face was mapped during the development of the tunnel, orientated

laterally at the midpoint. Data from this face was used for the calculation of initial CLD values, but not for the actual modeling, allowing it to be used for comparison to stochastic fractures through the same plane.

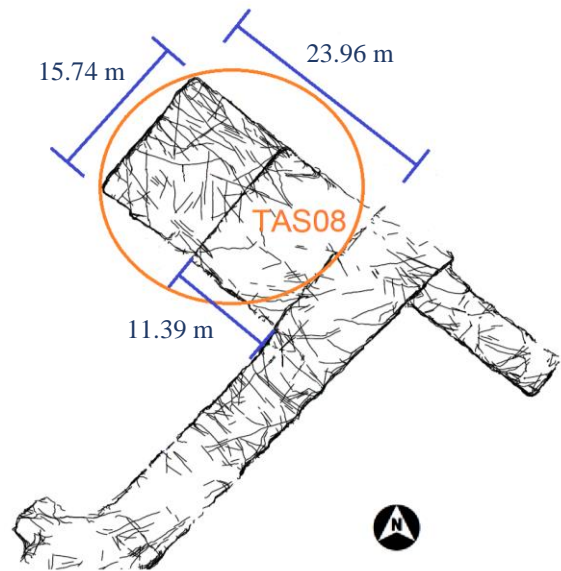


Fig. 1. Plan view of the Äspö TAS08 tunnel at the SKB Hard Rock Laboratory (courtesy SKB).

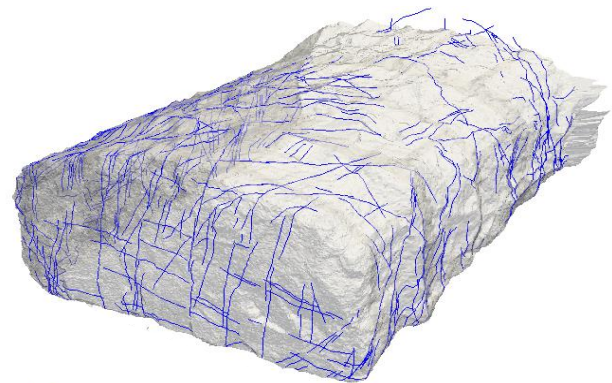


Fig. 2. Fracture traces mapped on the Äspö TAS08 tunnel walls.

The surface area of the tunnel is calculated as the sum of the products of measured wall and face. A surface area of 950 m² is calculated from the tunnel face, back, and two walls.

4.1. Fracture orientation

Fractures mapped from the Äspö TAS08 tunnel walls are non-planar. Fracture traces, including those from the intermediate round tunnel face, were assigned strike and dip values during mapping and were analyzed for grouping using DIPS (Rocscience, 2015). Interpretation of the resultant stereonet yielded four major fracture groups; a fifth 'random' group was included to allow for representation of all fractures during modeling. The poles of the input traces and defined fracture groups are shown in Figure 3, as plotted on a stereonet.

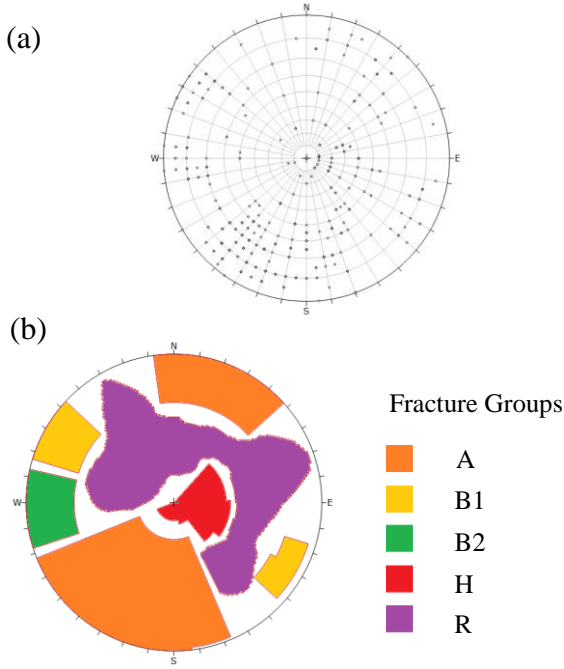


Fig. 3. Wulff stereonets of fracture traces in Äspö TAS08 tunnel showing (a) the poles of all mapped traces used for conditioning stochastic fractures and (b) the location of defined fracture groups.

DFN input parameters for orientation and fracture intensity are shown in Table 1. Fracture groups were divided into two subgroups based on size: up to 2 m, and larger than 2 m. CLD values were interpreted from the distribution of mapped traces. A CLD *dimension factor* was assigned independently for each subgroup. This allows for a reduced intensity in the small fractures as compared with the large fractures to account for bias associated with field mapped data that underestimates the true length of fractures traces.

4.2. Fracture intensity

When using CLD values to control fracture intensities in three dimensions, fractures can be seeded on a range of planes; these planes can be either predefined or randomized. For this study, CLD values were used to control the generation of stochastic fractures, as it allows for non-linear, probabilistically generated traces to guide the propagation of stochastic fractures. The strike to dip ratio of both deterministic and stochastic fractures was randomized from 0.25 to 4.0, with a mean of 1.0 (\bar{m}_{sd}). For each fracture group, using the height (z) of the domain and the mean trace length (\bar{m}_{tl}), the dimension factor (M) for the CLD values was calculated as:

$$M = z \div \left(\frac{\bar{m}_{tl}}{\bar{m}_{sd}} \right) \quad (2)$$

For fractures having a trace length of less than 2 m, the factor was divided by 4, and length thresholds were assigned. This compensated for the bias associated with data from mapped tunnel walls (Srivastava, 2006). Large fractures in a rock mass can be under-represented when mapped as traces that may not be completely exposed.

Small traces on walls could arise from either small or large fractures; they can also come from fractures induced through the excavation process, which are not intended to be modeled.

The CLD values used to define fracture intensities represent the slope of the curve on a log-log plot showing fracture intensity as a function of length. These values, calculated from the known traces, are shown in Figure 4. CLD values were assigned to each subgroup based on measured data and then adjusted using the given dimension factor to allow for the CLD to represent fracture intensity throughout the experimental volume.

Input intensity parameters were initially verified by comparing the P_{32} values for a representative equivalent volume (REV) and for the total experimental volume. The REV is determined as the product of the mapped surface area and mean length of fracture traces over that area. The mean length of fracture trace is 2.17 m. The REV is 2062 m³ and the experimental volume is 48,000 m³. The total surface area of all modeled deterministic fractures is used to compute P_{32} for the REV. Similarly, the total surface area of all fractures is used to compute P_{32} for the experimental volume. As the experimental volume is about 24 times the REV, the cumulative fracture surface area for these volumes is expected to exhibit the same ratio.

Table 1. Group orientation and intensity parameters used in DFN modeling of the Äspö TAS08 tunnel. Notation for size range is small (S), and large (L).

Group	Size range	Dip (degrees)	Dip direction (degrees)	Fisher constant (k)	L ₁ (m)	(P ₂₁) ₁ (1/m)	L ₂ (m)	(P ₂₁) ₂ (1/m)	CLD dimension factor
A	S	72	20	10	0.6	0.300	2	0.100	11.02
A	L	72	20	10	2.0	0.100	40	0.001	11.86
B1	S	89	121	38	0.5	0.070	2	0.020	9.86
B1	L	89	121	38	2.0	0.035	30	0.001	14.22
B2	S	78	86	90	0.5	0.070	2	0.020	9.50
B2	L	78	86	90	2.0	0.035	30	0.001	10.79
H	S	21	267	26	0.5	0.070	2	0.020	10.56
H	L	21	267	26	2.0	0.035	30	0.001	11.86
R	S	17	190	3	0.5	0.070	2	0.035	9.61
R	L	17	190	3	2.0	0.035	30	0.001	9.26

4.3 Fracture size

The mean fracture trace length of the dataset was 2.17 m, with a range from 0.228 to 15.3 m. The mean was the determining factor in the size-based classification of fractures. The determination of the minimum and the maximum lengths for each group was based on the original CLD representing mapped data. The minimum length for the small subgroups was set to 1.5 m, except for fracture group A, which had a minimum trace length for stochastic fractures of 1 m. The rationale for this was based on the distribution of traces, while considering the bias of over-representation of small traces, as group A showed a higher frequency of small traces and a lower minimum length compared with the other groups. The maximum trace length that limits the size of stochastic fractures was 25 m. This is 67% longer than the length of the largest trace in the dataset and reflects the TAC factor of 3 that was used for modeling. The CLD values used as input for DFN modeling for each subgroup are shown in Figure 5, before being adjusted by the calculated dimension factor. The minimum and maximum trace length settings are superimposed on this figure to demonstrate the range from which stochastic fractures are sampled.

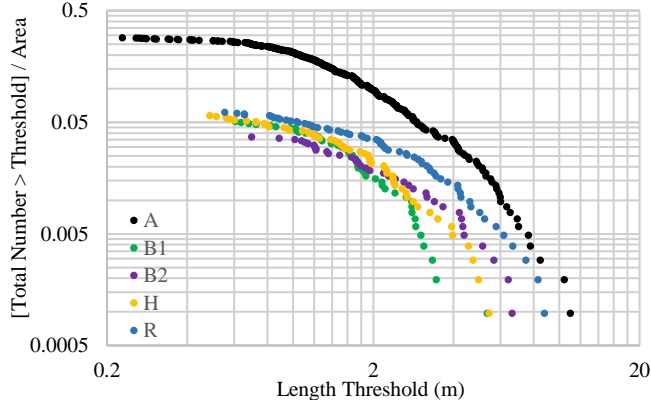


Fig. 4. Cumulative length distribution (CLD) for Äspö TAS08 tunnel dataset.

4.3. Fracture undulation

Fractures are undulated by honoring the mapped traces or stochastic traces that are generated by MoFrac. The settings for undulation defined increasing surface roughness for the five fracture groups. The fractal dimension ranged from 1.002 to 1.01. Fracture group A had the least roughness while fracture group R had the most. The second undulation parameter was set to the same scale, increasing with each fracture group. For the generation of stochastic traces, five iterations were used for each group.

4.4. Other DFN input parameters

Additional fracture attributes including strike to dip ratio, TAC factor, shape, joining and truncation probabilities can be provided as input. The probability of truncation was set to 1 between all fracture groups and the

probability of joining traces was set to 0 for this case study. Stochastic fractures were prevented from intersecting the tunnel wall mesh through a nudging procedure that shifts a stochastic trace down strike a distance of 5% of the trace length; this process continues until a stochastic trace does not intersect the tunnel wall.

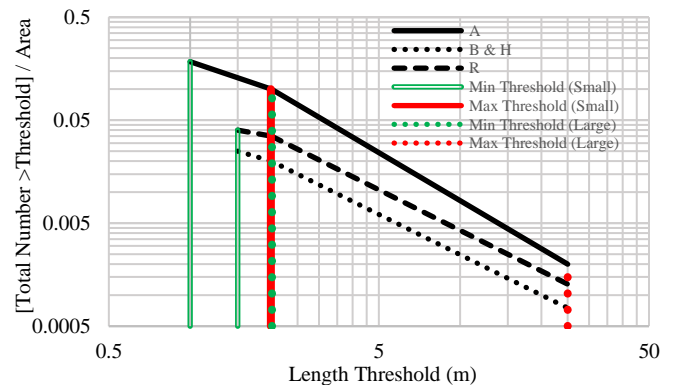


Fig. 5. CLD input used for generating DFN models of the Äspö TAS08 tunnel (before adjustment), with minimum and maximum length thresholds shown.

The strike to dip ratio, TAC factor, and shape of modeled fractures are group attributes, which are the same for each fracture subgroup and for both the deterministic and the stochastic fractures. The strike to dip ratio was set to a range of 0.25 to 4. This ratio considers the entire shape of the fracture and will not necessarily be reflected in a fracture that truncates. The TAC factor was set to a range of 1 to 3. DFN models were generated with rectangular and elliptical shapes separately for validation.

4.5. Model domain

An experimental volume of $40 \times 40 \times 30 \text{ m}^3$ ($l \times w \times h$) was defined to enclose the TAS08 tunnel. The tunnel wall mesh and the mapped lineaments were not rotated to match the X and Y axes. The volume extends from 410 to 380 m of depth and allows for about 10 m of unmapped space laterally from each side of the tunnel.

5. RESULTS

Three separate MoFrac generated DFN models representing the rock mass surrounding the Äspö TAS08 tunnel are shown in Figure 6. The models show three combinations of fracture shapes, rectangular, elliptical and randomly mixed. The DFN input parameters are used for comparison to, and validation of, the generated models. The orientation and location of individual deterministic fractures as well as overall group orientations, intensities and size distributions were analyzed quantitatively and compared to input values. The undulation parameters and geometric attributes were analyzed qualitatively by visual comparisons between both types of fractures and their traces along defined planes.

MoFrac can generate metrics that allow for quantitative assessment of the orientation, location, and size of all fractures generated. The metrics directly compare modeled deterministic fractures to the input dataset, and a VTK (Kitware, 2017) file is generated that shows all fracture intersections with a defined mesh. This mesh can be imported as an object or defined manually for modeling. For the analysis of the DFNs generated in this study, the TAS08 tunnel wall mesh was used. This facilitates a comparison ensuring that deterministic traces are being honored and there are no stochastic fractures that intersect surfaces where mapping has occurred. The intersections of modeled fractures with the surface of the tunnel walls are shown in comparison to the mapped traces on the same surface in Figure 7.

5.1. Fracture orientation results

The orientations of modeled fractures were first inspected on a stereonet. Figure 8 compares the stereonet from deterministic fractures modeled using both shapes with the stereonet showing all 5873 stochastic fractures from the final DFN model. A cursory visual inspection demonstrates the similarities in orientation compared with group orientations of the mapped fractures (Figure 3). The orientations are also reported in Table 2 based on analysis through visualization of orientations on a stereonet and by using the reported dips and dip directions from MoFrac.

5.2. Fracture intensity results

Fracture intensity validation was performed in two stages, first by comparison of the overall P_{32} value for deterministic fractures, based on the REV, to the P_{32} value for the entire set of generated fractures based on the experimental volume. The experimental volume is 24 times larger than the REV and thus the ratio between the cumulative fracture surface areas of both volumes is expected to also be 24:1. The P_{32} values for the deterministic fractures were calculated for each size grouping as follows; rectangular and elliptical fractures had P_{32} values of 0.69 m^{-1} and 1.21 m^{-1} respectively and 1.02 m^{-1} for the mixed fractures. For the full DFN including stochastic fractures, a P_{32} of 1.08 m^{-1} was realized. Due to differences in truncation between shapes, the rectangular fractures had a higher degree of truncation which results in a lower P_{32} value.

The CLD values needed for stochastic fracture generation were derived from the mapped fracture length distribution. The output of the DFN model is measured in terms of fracture surface area. As CAD output values reflect the dimension factor used, the size distribution of modeled fractures must be modified for comparison to the CLD values. The surface areas must first be resolved to fracture lengths, and by dividing out the dimension factor used for conversion a CLD is generated. CLD and CAD curves were used to compare fractures from all five fracture groups combined, and are shown in Figures 9 and 10 respectively. As the probability distributions that affect

fracture geometry have mean values that define an elliptical disc or rectangular plane, the fracture surface area can be converted to a maximum trace length through simple algebra,

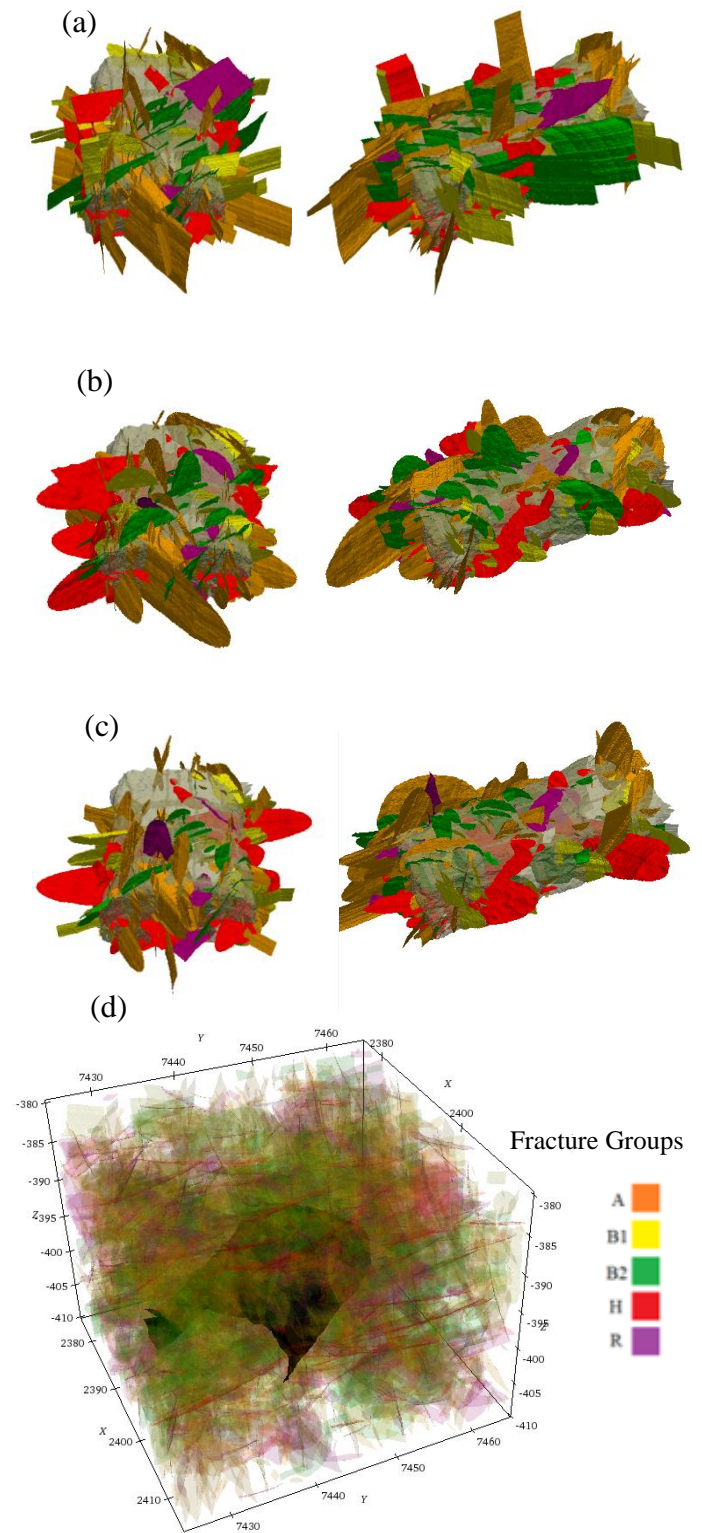


Fig. 6. DFN model of rock volume surrounding Äspö TAS08 Tunnel, showing deterministic fractures only, with fractures modelled as (a) rectangles, (b) ellipses, (c) mixed, and (d) all fractures transparently over tunnel wall.

$$L = 2 \cdot \sqrt{\frac{A}{\pi}} \quad (3)$$

and,

$$L = \sqrt{A} \quad (4)$$

where L is the maximum trace length and A is the reported fracture surface area. Eq. 4 applies to elliptical fractures and Eq. 5 to rectangular fractures. By modifying the CAD curve, an approximation of the representative CLD curve is determined which can be compared directly with input values. The use of both CLD and CAD distributions ensures that stochastic fractures honor the deterministic fracture intensities and that both types of fractures are honoring the input intensity values.

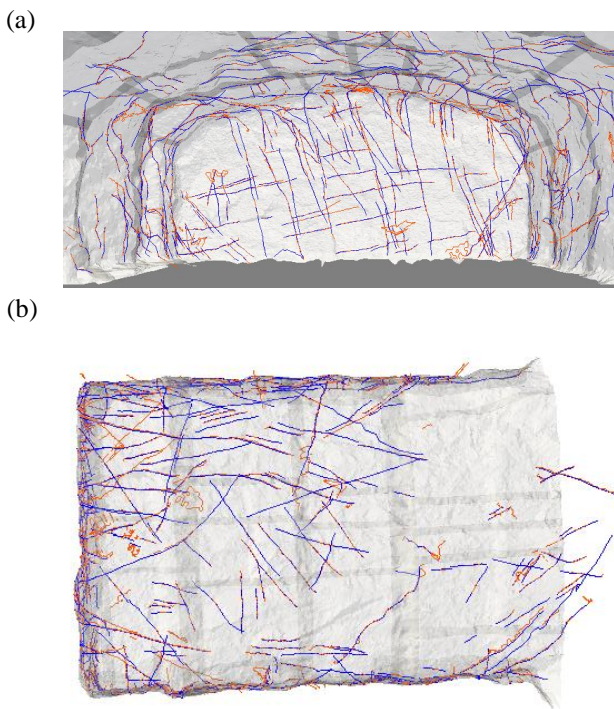


Fig. 7. Intersections of modeled fractures (orange) and mapped fracture traces (blue) with TAS08 tunnel walls on (a) the back face and (b) the roof.

Table 2. Comparison of mean input and output fracture group orientations.

Fracture Group	Input fracture orientation			Deterministic fractures			Deterministic fractures			Deterministic fractures			Stochastic fractures		
				Rectangular			Elliptical			Mixed shapes			Mixed shapes		
	stereonet			stereonet			MoFrac reported			MoFrac reported			MoFrac reported		
	Dip	Dip direction	k	Dip	Dip direction	k	Dip	Dip direction	k	Dip	Dip direction	k	Dip	Dip direction	k
A	72°	20°	10	74°	22°	9	78°	31°	9	74°	19°	9	70°	20°	11
B1	89°	121°	38	90°	127°	95	89°	126°	76	80°	129°	25	83°	121°	43
B2	78°	86°	90	88°	105°	87	90°	102°	77	77°	87°	26	79°	86°	86
H	21°	267°	26	25°	286°	23	25°	285°	21	31°	276°	9	27°	265°	25

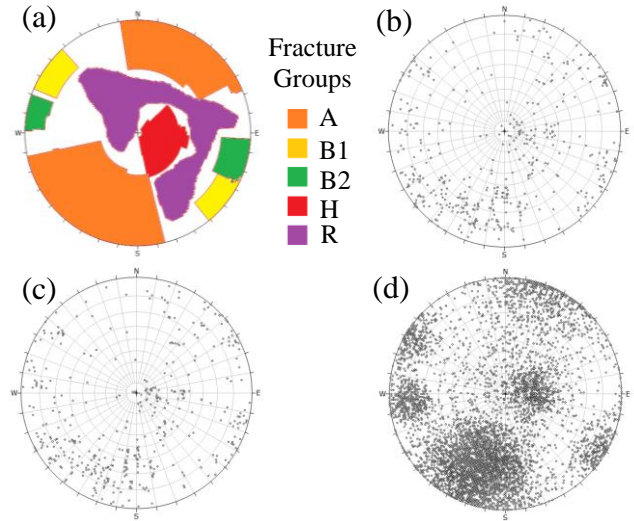


Fig. 8. Wulff stereonets of deterministic fractures modeled near Äspö TAS08 tunnel, showing (a) the location of defined fracture groups, and the poles of modeled (b) rectangular fractures, (c) elliptical fractures, and (d) randomly mixed fractures including stochastics.

5.3. Deterministic fractures

The metrics generated by MoFrac allow for a direct comparison of mapped fracture traces to the traces that a DFN model would create on the same. By analyzing the results of the metrics report, any misfits to the model can be identified and inspected.

The error in orientation is reported as an absolute value. The orientation error for each fracture group are weighted by the number of fractures, to give the mean error and associated standard deviation for the model. Results of the orientation error and a positional metric are presented in Table 3.

The metrics report considers the orientation and location of fractures by comparing input with output attributes. The position of a fracture trace is compared spatially with the location of the input trace in three dimensions, using a method analogous to calculating the longitudinal root mean square error (LRMSE) (Anderson *et al.*, 2014).

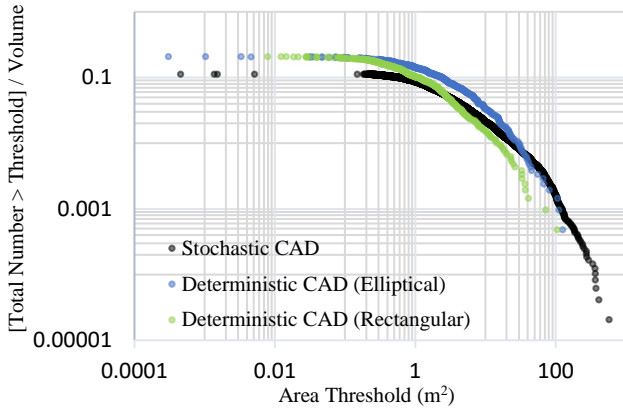


Fig. 9. Comparison of CAD curves for deterministic (by shape) and stochastic (mixed shape) fractures generated in the Äspö TAS08 tunnel DFN model.

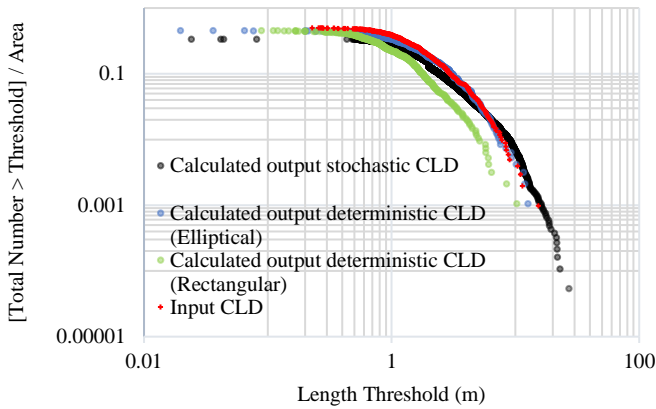


Fig. 10. Comparison of CLD curves for input, stochastic and deterministic outputs. Output CLD values are resolved to lengths from calculated surface areas and normalized to a horizontal plane by removing the dimension factor used to express intensity with depth.

Table 3. Metrics analysis of DFN showing error associated with length, orientation and position of deterministic fractures in respect to their traces across the same surface.

Attribute, Metric	Rectangular		Elliptical		Mixed	
	Mean error	Standard deviation	Mean error	Standard deviation	Mean error	Standard deviation
Dip Direction, Absolute Error	7.6°	8.4°	21.3°	16.6°	12.2°	11.4°
Dip, Absolute Error	6.4°	5.4°	12.9°	10.4°	10.7°	13.3°
Location, LRSME	0.65	0.25	0.30	0.23	0.55	0.31

5.4. Fracture geometry

Geometric attributes of generated fractures are considered qualitatively. A range in strike to dip ratios creates a variety in fracture shapes regarding the aspect ratio, however all fractures should display a convexity. Fractures are shown in Figure 11 that demonstrate the variety in fracture geometry that MoFrac utilizes to create a DFN with a realistic appearance, as shown in detail with single fractures from each group. The degree of assigned roughness increases from (a) to (e).

A DFN can be inspected by slicing on an inspection plane. The geometry of these traces can be compared with the field mapped fracture traces by comparing planes cut at different positions, but with the same orientation, within the domain. In the case of the Äspö TAS08 dataset, an intermediate face was mapped during the development of the tunnel. This allows for a direct comparison between the actual mapped fractures at this location to the traces of the stochastically generated fractures that pass through it. Figure 12 shows the location of the inspection plane with respect to the tunnel and shows both the mapped traces across this plane and the traces generated by MoFrac.

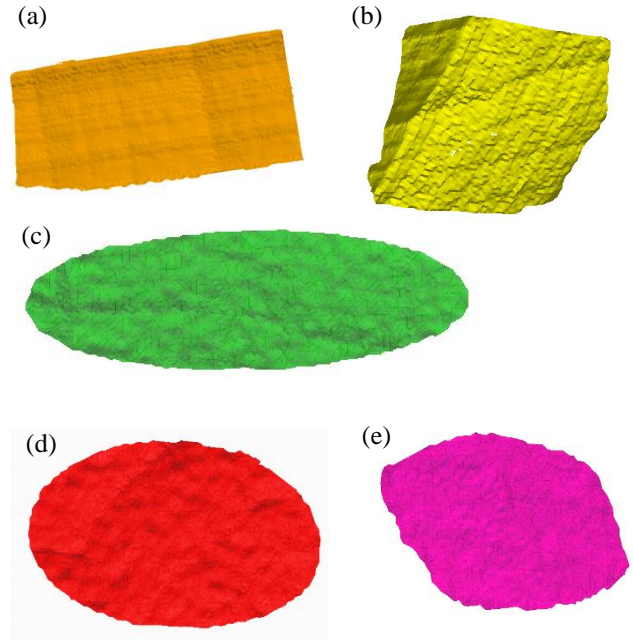


Fig. 11. Examples of fracture shape and undulation from each fracture group (a)-(e). Fracture roughness increases with each group.

Apart from the visual comparison, P_{21} value were calculated based on the total number of traces across the inspection plane. The overall P_{21} for the deterministic traces on the intermediate face is 0.79 m^{-1} and for the deterministic traces across the inspection plane was calculated as 0.94 m^{-1} . The intensities of generated fractures were modified from the mapped intensities in two ways. The number of small fractures were reduced, and those with lengths under 1 m were eliminated

entirely. Large fractures were generated with a simulated trace length up to 25 m. The longest mapped trace on the intermediate face ($15.74 \times 7 \text{ m}^2$) was 6.8 m. For this reason it is to be expected to calculate a higher P_{21} value for the stochastic fracture traces across the inspection plane than is calculated for mapped traces, in the case of this model the P_{21} value is 19% higher for the stochastic traces compared to the mapped traces.

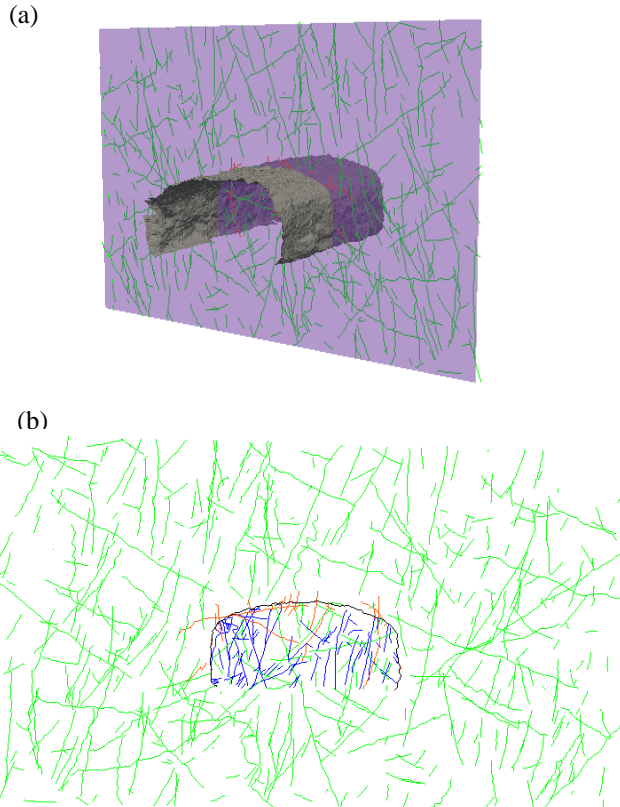


Fig. 12. Stochastic traces across the plane defining the intermediate face of the TAS08 tunnel. (a) The intersection of the inspection plane with the tunnel walls. (b) The entire inspection plane showing modeled deterministic (orange) and stochastic (green) fracture traces with known mapped fracture traces from the intermediate face (blue).

Areas where mapped data was not complete, such as the tunnel floor, were analyzed by comparing the fractures modeled inside the tunnel when viewed from below. Figure 13 shows the interior of the tunnel both with only deterministic fractures and with stochastic fractures included. It can be seen that a large degree of infilling has occurred, while not generating any additional traces on the tunnel wall. This demonstrates the effectiveness of the nudging technique to control the location of stochastic fractures relative to the tunnel walls, preventing unwanted intersections.

The degree to which known data, derived from mapped fracture traces, is honored, is shown through analysis of orientations, intensities and location. Elliptical shaped fractures tend to honor the location of the trace along the entire path better than rectangular shaped fractures.

Conversely rectangular fractures tend to honor input orientation to a higher degree than the elliptical shaped fractures. Figure 14 shows the ten worst fit fractures from the models presented. The five worst fit fractures based on location are shown for the rectangular shape and the five worst fractures based on orientation are shown for the elliptical shape.

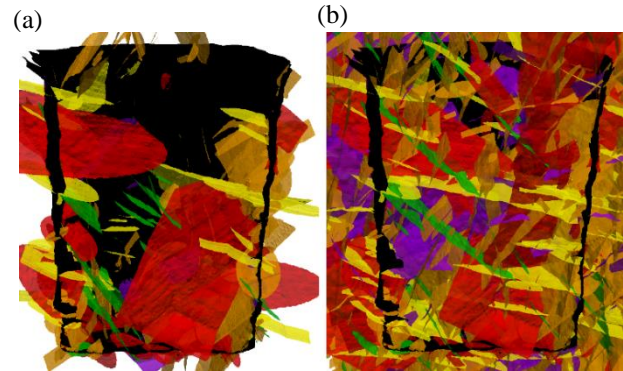


Fig. 13. View from below the tunnel mesh showing (a) deterministic fractures only and (b) infilling due to stochastic fractures.

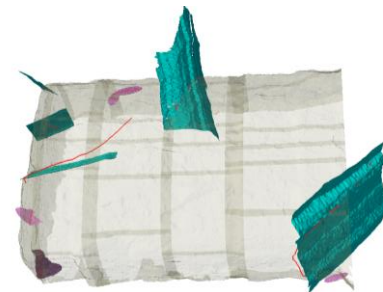


Fig. 14. The ten worst-fit fractures measured during modelling. Rectangular fractures shown in teal and elliptical fractures shown in pink with mapped fracture trace in red.

6. CONCLUSIONS

This case study and validation demonstrates the ability of MoFrac to generate realistic and conditioned DFN models. Using data mapped from SKB's Äspö TAS08 tunnel, DFN models were generated and presented. The DFN models were analyzed quantitatively and qualitatively regarding accuracy and appearance.

DFNs generated by MoFrac are intended to honor information regarding the fractured rock mass used as input. Stochastic fractures are conditioned to known statistical data and are generated in areas of the experimental volume that have not been mapped, or where data has not been provided. The stochastic fractures generated match the intensities and orientations of the deterministic fractures from which they are derived.

Orientations for deterministic fractures are shown to reflect the assigned input values with an accuracy of 90% or greater in terms of groups and with an accuracy of 80% or greater in terms of individual fractures. As modelled

fractures are undulated during propagation and the reported orientation is determined from the completed fracture, it is expected that there would be an error associated with orientation when considered on a fracture by fracture basis. By first considering the reported orientations by group, given in Table 2, where the associated absolute error is generally below 10°, and comparing them to the mean error when considering individual fractures, which was calculated to be as high as 21.3°, the effect of undulation is evident. This demonstrates that overall, the undulation parameters are affecting orientation on individual fractures but do not affect group orientations as significantly. This is due to an averaging of the associated error over the entire group. This is expected, as the known orientation values of a fracture are location dependent.

DFNs generated using MoFrac can be integrated in numerical models to solve geo-engineering problems related to excavation stability, ground control, drilling and rock fragmentation, as well as related studies including groundwater flow, mass transport, induced fracturing.

7. ACKNOWLEDGEMENTS

Appreciation is given to SKB for providing the dataset for modeling. MoFrac has been developed with support from the NWMO (Nuclear Waste Management Organization), Rio Tinto, and NSERC (Natural Sciences and Engineering Research Council) CRD grant CRDPJ 470490-14. Additional funding has been provided through the Ontario Trillium Scholarship and the NOHFC (Northern Ontario Heritage Fund Corporation).

REFERENCES

- Anderson, D.L., D.P. Ames & P. Yang, 2014. Quantitative Methods for Comparing Different Polyline Stream Network Models. *Journal of Geographic Information System* (6). pp. 88-98.
- Dershowitz, W. & H. Herda, 1992. Interpretation of fracture spacing and intensity. *Rock Mechanics*. Tillerson & Wawersik (eds), Rotterdam. pp. 757-766.
- Farahmand, K., I. Vazaios, M.S. Diedrichs & N. Vlachopoulos, 2015. Generation of a Synthetic Rock Mass (SRM) Model for Simulation of Strength of Crystalline Rock using a Hybrid DFN-DEM Approach. *EUROCK 2015 & 64th Geomechanics Colloquium*. Schubert (ed.)
- Jing, L. & O. Stephansson., 2007. Discrete Fracture Network (DFN) Method. Chapter 10 in *Developments in Geotechnical Engineering*. pp. 365-398.
- Kitware, 2017. The Visualization Toolkit, (<http://www.vtk.org/>)
- Long, J.C.S., P. Gilmour & P.A. Witherspoon., 1985. A model for steady fluid flow in random three-dimensional networks of disc-shaped fractures. *Water Resources Research* (21). pp. 1105-15.
- Lei, Q., J.P. Latham & C.F. Tsang, 2017. The use of discrete fracture networks for modeling coupled geomechanical and hydrological behaviour of fractured rocks. *Computers and Geotechnics* (85). pp. 151-176.
- Lei, Q., J.P. Latham, J. Xiang, C.F. Tsang, P. Lang & L. Guo, 2014. Effects of geomechanical changes on the validity of a discrete fracture network representation of a realistic two-dimensional fractured rock. *International Journal of Rock Mechanics & Mining Sciences* (70). pp. 507-523.
- Li, Y. & R. Huang, 2015. Relationship between joint roughness coefficient and fractal dimension of rock fracture surfaces. *International Journal of Rock Mechanics & Mining Sciences*. 75, pp. 15-22.
- Macciotta, R. & C.D. Martin, 2015. Remote Structural Mapping and Discrete Fracture Networks to Calculate Rock Fall Volumes at Tornado Mountain, British Columbia. *49th US Rock Mechanics/Geomechanics Symposium, ARMA*.
- Rocscience, 2015. DIPS, Ver. 6.0.17. Available at: <https://www.rocscience.com/rocscience/products/dips>.
- SKB, 2016. Äspö Hard Rock Laboratory Annual Report, 2015. *Technical Report TR-16-10. Swedish Nuclear Fuel and Waste Management Co.* July 2016.
- Srivastava, M., 2002. Probabilistic Discrete Fracture Network Models for the Whiteshell Research Area. *Report No: 06819-REP-01200-10071-R00, Ontario Power Generation, Toronto*. February 2002.
- Srivastava, M., 2006. Field verification of a geostatistical method for simulating fracture network models. *Golden Rocks 2006, The 41st US Symposium on Rock Mechanics (USRMS), ARMA*.
- Srivastava, M., P. Frykman & M. Jensen, 2004. Geostatistical Simulation of Fracture Networks. *Geostatistics Banff 2004*. pp. 295-304.
- Vazaios, I., M.S. Diedrichs & N. Vlachopoulos, 2015. A study of the geometrical scale-dependency of fractured rock masses using LIDAR scanning: The case study of Brockville Tunnel. *ISRM, 13th International Congress on Rock Mechanics, Montreal 2015*.
- Vazaios, I., M.S. Diedrichs, N. Vlachopoulos & M.J. Lato, 2014. LIDAR as input for Discrete Fracture Networks: A comparison of automated manual joint mapping using scanned surfaces. *Canadian Geotechnical Society, GEO Regina 2014*.